ISSN 2176-5480

22nd International Congress of Mechanical Engineering (COBEM 2013)
November 3-7, 2013, Ribeirão Preto, SP, Brazil

ANALYSIS OF THE RESIDUAL STRESS INDUCED BY PEEN FORMING IN ALUMINUM ALLOY SPECIMENS

Dalla Pacce, P.H.,
Escola Politécnica da Universidade de São Paulo
pedrodallapacce@gmail.com

Martins, F.P.R.
Escola Politécnica da Universidade de São Paulo
flavius.martins@poli.usp.br

Fleury, A.T.
Centro Universitário da Fundação Educacional Inaciana (FEI)
Universidade de São Paulo
agfleury@fei.edu.br
agenor.fleury@poli.usp.br

Abstract. *Peen forming is a cold work process based on the application of a regulated blast of small round steel shots on the surface of a metallic plate or panel. The local plastic deformations caused by the impacts give rise to a thin compressive residual stress layer that stretches the worked surface. Therefore, to give a piece a predefined shape, it is necessary to properly control the peen forming process variables, for which a reference model for the measurements is required. Aiming at developing a computer-aided tool for planning peen forming processes for the aeronautical industry, a series of experiments have been carried out on test rectangular plates of aluminum 7050 and 7075 alloys, encompassing the variation of four relevant variables of the process– shot diameter, impact velocity, coverage (% of the surface area affected by the shots) and preloading. For each shaped specimen, the blind-hole drill method was applied to determine the residual stress distribution at mid span, a coordinate machine was used to measure the curvature of the plates after being peen formed, image processing techniques were applied to estimate both the coverage and the radii of the shot printings and the average velocity of impact was estimated by a simplified theoretical function that depends on the shot average printing radius. In order to evaluate the quality of the residual stress measurements, an analytical model for the peen forming process was tested against the experimental data, and statistical techniques concerning error analysis, were applied to estimate the degree of adherence of experimental data to the referred model.*

Keywords: *peen forming, residual stress distribution, plastic layer, blind-hole method, propagation of errors.*

1. INTRODUCTION

Aluminum alloys, specially the SAE 7XXX family, have widespread usage in aircraft construction since its mechanical and structural properties conform very well to the aeronautical design requirements. Actually, at least 80% of a modern airplane weight is aluminum, being the SAE 7050 and 7075 alloys the ones most used in structural components.

Machining, based on a 4 or 5 axis CNC milling machine, is traditionally used to manufacture those components from prismatic blocks. Albeit this class of process produces components with high reliability, it also generates material loss, which, sometimes, reaches 95% of the blank. Moreover, huge surfaces with saddle points, such as wing panels, sometimes cannot be generated through machining due to the topological and geometrical characteristics of the CNC machines. Such difficulties can be advantageously overcome if peen forming is adopted to manufacture those components.

Peen forming consists of a non-destructive advanced manufacturing process. It requires a machine that shoots metallic, ceramic or glass spheres on the surface of the plate or panel intended to be shaped. The continuous impacts dent the target, and, this way, generates superficial plastic deformation in the material. The interaction of the permanently deformed layer (plastic zone) with the surrounding elastic zone causes the piece to elastically bend. Furthermore, the compressive residual stress applied in the surface is responsible for the significant increase observed in its fatigue resistance.

Despite the advantageous characteristics cited above, lack of robust analytical models to relate the shot dynamics with the piece deformation make peen forming process planning a very difficult task. So, empirical methods have been adopted to estimate the shot characteristics necessary to produce a given curvature on the piece. The most used technique is the so-called Almen method (Niku-Lari, 1981a; Niku-Lari, 1981b), in which the deformation of a standard steel strip (Almen strip) submitted to a given shot blast is adopted as a measure of the peen forming intensity.

ISSN 2176-5480

The development of an analytical model that effectively describes peen forming has been pursued by a large group of researchers. A common approach to analyze the effects of shot peening relies on the application of elements of Theory of Plasticity and Contact Mechanics.

Al-Obaid (1995), for instance, proposed an analytical model to estimate the compressive layer depth using measures of the indentation caused by the shot blast. Old studies of the stress distribution in contact of two non-conforming solids, without adhesion (Johnson, 1985), are a good starting point to the comprehension of the peen forming phenomenonology. Considering that Hertz's theory and Boussinesq's potential functions (Timoshenko, Goodier, 1970) requires as hypothesis that the loading is quasi-static, peen forming models based on this analysis are relatively poor approximations to the real phenomenon, which involves the dynamical interaction between the shot and the effect due to impact of the spheres. However, even adopting such simplified models it is possible to estimate both the stress profile and the plastic layer depth.

More modern studies rely on Finite Elements Methods to determine shot peening effects (Levers and Prior, 1998; Meo and Vignejevic, 2003). Although generating results close to the empirical data, these models are numerical; therefore, hard to apply in the logistics of manufacturing. Meguid et al. (1999a; 1999b), for instance, developed a shot peening mathematical model using dynamic elasto-plastic analysis related to single and double impact events. However, extension of such a model to the overall shot area implies in a too-high computational cost.

Due to the limitations of the analytical models, experimental data is often required to explain the phenomena involved in peen forming. Indeed, several authors (Tatoon, 1986; Watanabe and Hasegawa, 1997; Evans, 2002) stress that the use of experimental data to synthesize peen forming models is the only feasible approach capable to provide proper information for peen forming process planning.

To develop a computer aided peen forming process planning tool suitable for the national aircraft industry, a team of IPT (Instituto de Pesquisas Tecnológicas do Estado de São Paulo) carried on a series of experiments designed to elicit relationships amongst the peen forming variables. Even though some of the results derived from this project were previously published in articles and proceedings (Almeida et al., 2008; Delijaicov et al., 2010; Vieira et al., 2010; Fleury et al., 2009; Fleury et al., 2011), a significant amount of data still remains unanalyzed.

In this article it will be investigated the adherence of measured residual stress data induced in aluminum alloy plates to the predictions made by the classical models of Al-Obaid and Watanabe and Hasegawa, which were previously validated by experiments performed on steel work pieces.

2. EXPERIMENTAL SET UP

The peen forming experiments encompassed variations of 4 relevant variables of the process – shot granulometry, impact shot velocity, surface coverage (hit surface area per total surface area ratio) and pre-loading. The specimens used in the experiments were 7050 and 7475 aluminum alloy plates with sizes of 400mm×50mm and thicknesses of 2mm, 5mm, 10mm and 15mm.

To avoid the huge number of parameters' combinations, a 4-variable-matrix, containing the most relevant parameters, was created and a fractional factorial design of experiments was implemented. Those experiments combined 3 levels for shot granulometry (S230, S550 and 1/8"), 3 levels for impact shot velocity ('High', 'Medium' and 'Low'), 2 levels for surface coverage ('High' and 'Low') and 2 levels for preloading (null or 90% of the material yield strength'). The designed test matrix, covering 144 different combinations between the process variables and the specimens' characteristics, is shown in Table 1. It must be emphasized that each experiment was replied for 3 specimens, giving rise to a total of 432 experiments.

Table 1. Test matrix

Thickness (mm)	Alloy	Mean shot diameter (mm)	Shot velocity level	Coverage (%)	Preloading	Number of combinations
2	7050	0,7	low	low	nil	24
	7475		medium	high	90%Y	
			high			
5	7050	0,7	low	low	nil	48
	7475	1,3	medium	high	90%Y	
			high			
10	7050	1,3	low	low	nil	48
	7475	3,2	medium	high	90%Y	
			high			
15	7050	3,2	low	low	nil	24
	7475		medium	high	90%Y	
			high			

The specimens were peen formed by the IPT Metallurgical Laboratory using a CNC shot peening equipment especially designed to meet the needs of the experiments. Suitable auxiliary and measurement instruments were also used to obtain adequate values for the parameters of the process.

ISSN 2176-5480

By properly regulating the air pressure and the shot metering valve opening, three distinct levels of shot velocity could be set up for each of the three types of shot used in the experiments.

The required coverage levels were attained by experimental procedures aimed at characterizing the distribution of the hit plate areas according to distinct nozzle feed rates (Almeida et al., 2008).

Preloading was applied to the specimens by a mechanical device inserted in the shot peening chamber machine (Fig. 1a) whereas surface distribution stresses were measured by a set of unidirectional and three axial strain gauges connected to a signal acquisition system (AqDAnalysis, from Lynx Tecnologia).

The average levels of shot impact velocity were controlled using a mechanical device based on two parallel rotating discs – the 'reference disk', supplied with an angular scale, and the 'filter disk', exhibiting a small orifice near its border. As described by Clausen e Stagenberg (2002), when the angular velocity of the disks is known, the average shot velocity can be estimated from the angle between the two major zones printed by the shots on the reference disk (Fig 1b).

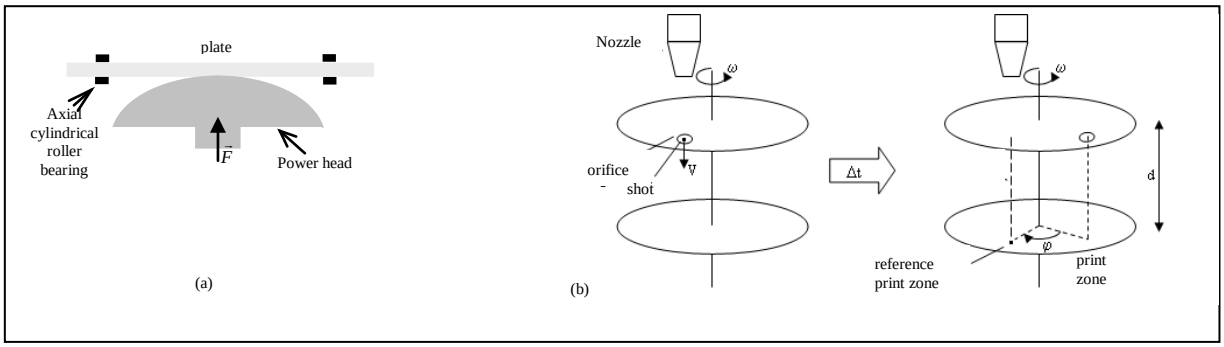

Figure 1. Auxiliary devices: (a) pre-loader; (b) mechanical instrument to estimate the shot velocity.

More accurate estimates of the impact shot velocity and of the plate coverage were achieved by evaluating the geometrical characteristics of the prints caused by the impacts against the plate; such measurements were carried on through the application of image analysis tools on amplified images of the specimens' surfaces, as it will be explained in section 3.

The final curvatures of the specimens submitted to peen forming were measured with a coordinate machine (QM353 model, from Mitutoyo Co).

Measurements of residual stresses induced on the specimens by the peen forming process were made both on the surface and along the depth of the plastic layer. Superficial residual stresses were measured by an X-ray diffractometer (model XRD-6000, from Shimadzu Co), equipped with a goniometer to properly orientate the samples of the specimens. The blind-hole drill method (Valente et al., 2005) was applied to measure the residual stress according to layer depth. For this, it was necessary to glue strain gauge rosettes around small holes (1mm diameter) made on the specimen by a high precision drill (model RS-200, from Vishay Precision Group, Inc) and progressively increasing the depth of the hole and collecting the strain gauges measurements; then, using the software tool H-Drill (from Vishay Precision Group, Inc), residual stresses were calculated and stored on a spreadsheet for analysis.

3. ANALYTICAL METHODS

On this article, analysis focuses the relationship between the estimated parameters of the peen forming processes and the residual stress measurements issued by the blind-hole method. The intent is to investigate the degree of coherence between those data and reference models (Al-Obaid, 1995; Watanabe and Hasegawa, 1995) that were previously validated for steel shot peened work pieces.

The analysis is based on the experimental data concerning to the test specimen named CP192, a 7050 aluminum alloy rectangular plate with sizes of 400mm×50mm×5mm. Such specimen was submitted to blasting with carbon steel shot S550 (1.94mm mean diameter) that hit its surface at a velocity of 14m/s, approximately, giving rise to a coverage of 60%. No preloading was applied to this specimen during the experiment.

In order to be implemented, the analytical models of Al-Obaid and Watanabe and Hasegawa require good estimates of both the impact shot velocity and the indentation depth due to the impacts. As no precise, specific instrumentation was used to measure those variables, we adopted an indirect measurement method based on image analysis. Therefore, 25× magnified images of the peen formed work pieces surface were grabbed by an image acquisition system composed by an image frame-grabber (model PC2-Vision, from Coreco Imaging Co), a CCD video camera (model CVM10BX, from JAI Inc), a zoom lens (model Zoom 7000, from Navitar Inc), an ellipsometer (model 432A4, from Rudolph Instruments Co.) and two LED ring illuminators.

ISSN 2176-5480

Although automatic computer vision methods could provide reasonable estimates for the coverage in cases of low covered images (Vieira et al., 2010), attempts to implement a robust computer vision method to estimate the average diameter of the prints on images like the one shown in Fig. 2a, were not successful. Instead, we used an interactive algorithm that constructed a circle through three points specified by a human operator, who was the responsible for identifying the borders of the shot prints, as indicated in Fig. 2b.

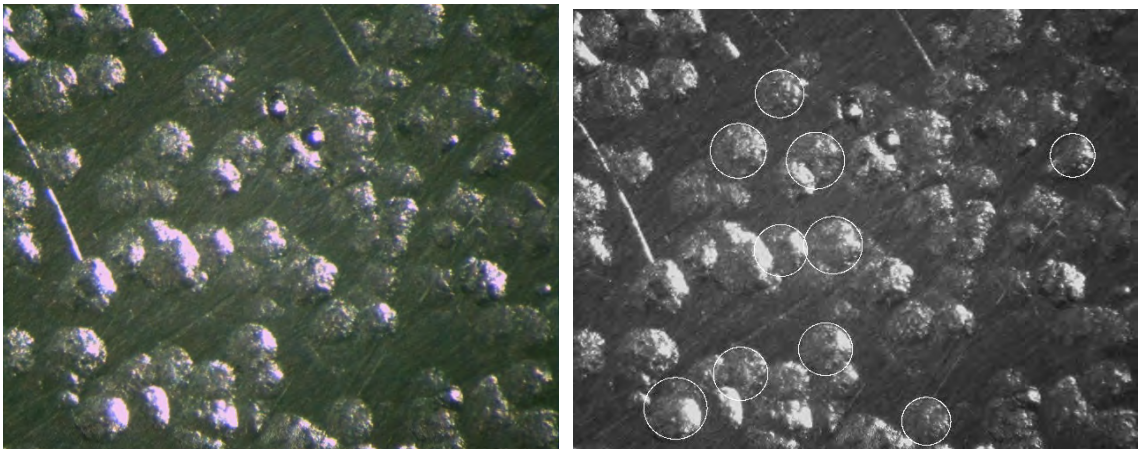

Figure 2. (a) Image of the shot peened surface of a plate; (b) identified shot print zones.

The statistics of the shot print diameters for the experiments made with CP192 were based on100 samples of circles identified on 10 images according to the procedure described in the above paragraph, i.e., fitting a circle through three points defined by a human operator. As a result, the estimated shot print mean radius was R= 0.97mm.

The mean impact shot velocity was estimated using the equation of single shot impacts, as presented in Evans (2002), i.e.:

$$v_0 = \left[\frac{2.8 a_f^4 \pi \bar{\sigma}_y}{2mr} + \frac{14.1 \pi^2 a_f^3 \bar{\sigma}_y^2}{3m} \left(\frac{1-\nu_1^2}{E_1} + \frac{1-\nu_2^2}{E_2} \right) \right]^{1/2} \tag{1}$$

In the above equation, ν_1, E_1 and ν_2, E_2 are, respectively, the Poisson's ratio and the Young's modulus of the workpiece and the shot, $\bar{\sigma}_y$ is the aluminum alloy Von Mises yield stress, r is the shot radius and a_f is the final indentation radius (see Fig.3), estimated from the measured radius prints of the same circles previously identified in the images. Using this method, it was estimated that $v_0 \approx 14.0\, m/s$.

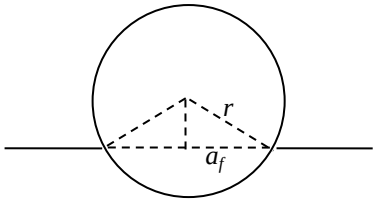

Figure 3. Relationship between the shot radius and the print radius.

The theoretical residual stress and plastic layer depth are, both, functions of several parameters encompassing different levels of uncertainty, since they are estimated from heterogeneous methods. Therefore, it is necessary to apply a technique of uncertainty propagation to properly estimate the uncertainty of the dependent variables. Such technique consists of writing the uncertainty of the focused function $f = f(a_1, \ldots, a_n)$ in terms of their partial derivatives, as indicated below:

$$\sigma_f = \sqrt{\left(\frac{\partial f}{\partial a_1} \right)^2 \sigma_{a_1}^2 + \ldots \left(\frac{\partial f}{\partial a_n} \right)^2 \sigma_{a_n}^2} \tag{2}$$

The method of uncertainty propagation mentioned above was extensively used in the data analysis, as it will be presented in section 4.

ISSN 2176-5480

4. RESULTS

The model used as the reference for this research was extracted from Al-Obaid's work and also from Watanabe and Hasegawa's (1995) article. Therefore, all the demonstrations that give rise to the equations used next can be found in the refereed articles.

Al-Obaid proposes the following equation to estimate the plastic-layer depth

$$\frac{h_p}{R} = 3\left(\frac{2}{3}\right)^{\frac{1}{4}}\left(\frac{\rho V_0}{\bar{p}}\right)^{\frac{1}{4}} \tag{3}$$

where h_p is the depth of the plastic zone, R is the shot radius, $\bar{p}$ is the average pressure caused by the impacts, is the shot density and V_0 is the mean velocity of impact.

According to Al-Obaid, $p = 3Y$,where Y=yield stress of the test specimen; so, substituting the proper parameters in the Eq.3, it yields h_p=0,5mm, in close agreement with the plastic zone depth value measured using the blind hole method, as it can be seen in the graphic of Fig. 4.

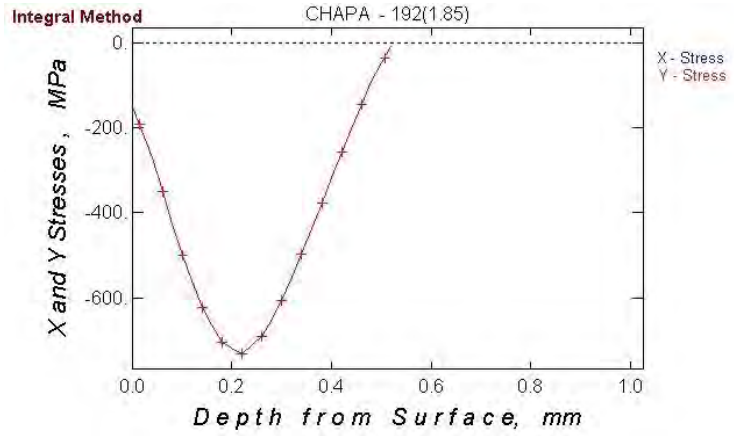

Figure 1. CP192 residual stress experimental profile

Al-Obaid (1995) describes the residual stress profile as a sum of three stress components in the peened surface. The interaction between the plastic layer and the elastic zone creates a *source stress*; also, the elastic zone reacts to the expansion of the plastic zone generating axial and bending stresses. Therefore, the resulting profile is given by:

$$\sigma_R = \sigma_B + \sigma_S + \sigma_{ax} \tag{4}$$

in which σ_R is the residual stress at depth z, σ_B is the bending stress, σ_{ax} is the axial stress and σ_S is the *source stress*.

Substituting the expressions for the component stresses in equation (4), yields:

$$\sigma_R(z) = \frac{E\varepsilon_m}{1-\nu}\left\{\frac{12\lambda}{\pi h}(1-\alpha)\left(\frac{h}{2}-z\right)C_1 + \frac{2\lambda}{\pi}C_2 - \frac{\epsilon(z)}{\varepsilon_m}\right\} \tag{5}$$

with

$$\epsilon(z) = \frac{\varepsilon_m}{2}\left\{\cos\left(\frac{z-\alpha h_p}{(1-\alpha)h_p}\right) + 1\right\} \text{ for } 0 \le z \le h_p \tag{6}$$

$$\varepsilon_m = \frac{2}{3}\frac{\pi h\delta}{\lambda L^2(1-\alpha)C_1} \tag{7}$$

$$\lambda = \frac{h_p}{h} \tag{8}$$

$$C_1 = C_2 - 2\lambda + \frac{4\lambda}{\pi}(1-\alpha)\cos\left(\frac{\pi\alpha}{2(1-\alpha)}\right) \tag{9}$$

$$C_2 = 1 + \sin\left(\frac{\pi\alpha}{2(1-\alpha)}\right) \tag{10}$$

where ε_m is the maximum deformation, E is the Young's Modulus for the panel, ν is its Poisson's ratio, z is the depth from surface and α is the fraction of h_p where the maximum stress occurs in thick targets. Also, h is the thickness of the target and L is its length.

ISSN 2176-5480

By using the aforementioned equations it is possible to obtain the residual stress profile at mid span of the CP192 test specimen (see Fig.2).

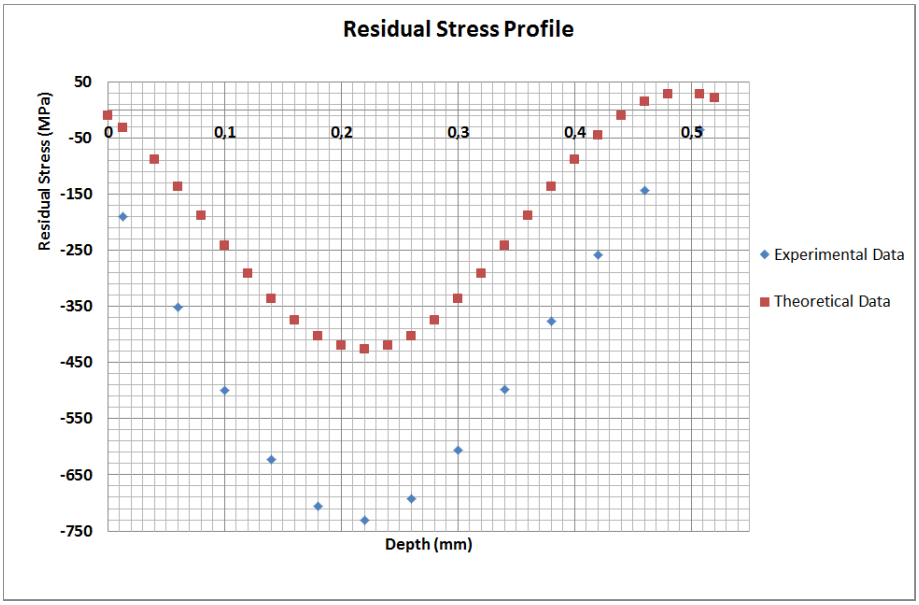

Figure 2. Comparison of the experimental and the theoretical residual stress profiles

The experimental residual stress profile shares resemblance with the predicted one, but exhibit evident discrepancies. In order to identify the variables that possibly give rise to much of these differences in the expected values, an uncertainty propagation technique was applied to the theoretical equations concerning the plastic layer depth and the residual stress profile estimations.

According to Eq. 3, the plastic depth is dependent on the shot radius and on the material density, impact velocity and yield stress of the plate, i.e.

$$h_p = h_p(R, \rho, V_0, \bar{p}) \tag{11}$$

Therefore,

$$\sigma_{h_p} = \sqrt{\left(\frac{\partial h_p}{\partial R}\right)^2 \sigma_R{}^2 + \left(\frac{\partial h_p}{\partial \rho}\right)^2 \sigma_\rho{}^2 + \left(\frac{\partial h_p}{\partial V_0}\right)^2 \sigma_{V_0}{}^2 + \left(\frac{\partial h_p}{\partial \bar{p}}\right)^2 \sigma_p{}^2} \tag{12}$$

By properly applying the derivative chain rule to evaluate σ_{hp} from Eq. 12, it was obtained, with the aid of Matlab(TM) symbolic toolbox, the following equation:

$$\sigma_{h_p} = \sqrt{\left(3\left(\frac{2}{3}\right)^{\frac{1}{4}}\left(\frac{\rho V_0^2}{\bar{p}}\right)^{\frac{1}{4}}\right)^2 \sigma_R^2 + \left(\left(\frac{3}{4}\right) R \left(\frac{2}{3}\right)^{\frac{1}{4}}\left(\frac{V_0^2}{\bar{p}\rho^3}\right)^{\frac{1}{4}}\right)^2 \sigma_\rho^2 + \left(\left(-\frac{3}{4}\right) R \left(\frac{2}{3}\right)^{\frac{1}{4}}\left(\frac{\rho V_0^2}{\bar{p}^5}\right)^{\frac{1}{4}}\right)^2 \sigma_{\bar{p}}^2 + \left(\left(\frac{3}{2}\right) R \left(\frac{2}{3}\right)^{\frac{1}{4}}\left(\frac{\rho}{\bar{p}V_0^2}\right)\right)^2 \sigma_{V_0}^2} \tag{13}$$

The above equation can be applied to determine the uncertainty of h_p estimation (i.e., σ_{hp}) and to evaluate the relative contributions of each independent variable in Eq. 13 to that uncertainty. As clearly stated in Eq. 13, the terms concerning the *a priori* uncertainty values of each independent variable are required to apply that equation to estimate the propagated uncertainty to the dependent variable. Those *a priori* estimations for the uncertainty values are listed in Table 2.

Table 1. *A priori* uncertainties assigned to the independent variables used in the theoretical models of h_p and σ_R

Variable	ρ	V_0	$\bar{p}$	R	h	L	δ	E	ν	z
Uncertainty	1%	50%	1%	1%	1%	1%	1%	1%	1%	1%

It must be emphasized that, for the cases which the required *a priori* uncertainty values were difficult to estimate, they were simply assigned according to reasonable heuristic criteria. For instance, it was assigned 50% to the *a priori* uncertainty of impact shot velocity, since this parameter was not measured, but estimated by an indirect method, as described previously.

ISSN 2176-5480

This way, by substituting the proper values of the *a priori* uncertainty parameters in Eq.13, it was estimated that σ_{hp} =0.1mm. Considering that h_p=0.5mm, the relative error is about 25% of the value predicted by the theoretical model.

After obtaining the uncertainty of the plastic layer depth, it was performed a sensibility analysis concerning the relative contribution of each parameter to the propagated uncertainty. This study has shown that the most relevant parameter is the shot radius followed by the impact velocity and at last, with the same relevance, the shot density and impact pressure. Therefore, changing the shot granulometry from S550 to S230 or 1/8" will affect the depth more than changing the pressure of shot ejection.

By replacing Eqs. 6, 7, 8, 9 in Eq.5, the following equation is obtained:

$$\sigma_R(z) = \left(\frac{2}{3}\frac{E\pi^2 h^3 \delta}{(1-\nu)(h_p L^2(1-\alpha)\left(\pi h\left(1+\sin\left(\frac{\pi\alpha}{2(1-\alpha)}\right)\right)+2h_p\left(-\pi+2(1-\alpha)\cos\left(\frac{\pi\alpha}{2(1-\alpha)}\right)\right)\right)}\right)\left(\frac{12h_p}{\pi^2 h^3}(1-\alpha)\left(\frac{h}{2}-z\right)\left(\pi h\left(1+\sin\left(\frac{\pi\alpha}{2(1-\alpha)}\right)\right)+2h_p\left(-\pi+2h_p(1-\alpha)\cos\left(\frac{\pi\alpha}{2(1-\alpha)}\right)\right)\right)+\frac{2h_p}{\pi h}\left(1+\sin\left(\frac{\pi\alpha}{2(1-\alpha)}\right)\right)-\frac{1}{2}\left(\cos\left(\frac{z-\alpha h_p}{(1-\alpha)h_p}\right)+1\right)\right) \quad (14)$$

Therefore, the residual stress depends on the Young's modulus E, the target thickness h, the resulting arc height δ, the depth z and the fraction of depth α where the maximum peak of compressive stress occurs relative to the target thickness the plastic layer depth h_p , which is a function of the impact velocity V_0, the shot density ρ and the target yield stress Y. Instead of introducing the plastic layer depth parameters in Eq. 14, h_p was assumed to be an independent variable; otherwise, Eq. 14 would depend on 9 variables, rendering it hard to differentiate. Hence, adopting this procedure σ_R was written as:

$$\sigma_R = \sigma_R(E, \nu, \delta, L, h, h_p, z) \quad (15)$$

$$\sigma_{\sigma_R} = \sqrt{\frac{\partial\sigma_R}{\partial E}^2 \sigma_E^2 + \frac{\partial\sigma_R}{\partial \nu}^2 \sigma_\nu^2 + \frac{\partial\sigma_R}{\partial \delta}^2 \sigma_\delta^2 + \frac{\partial\sigma_R}{\partial L}^2 \sigma_L^2 + \frac{\partial\sigma_R}{\partial h}^2 \sigma_h^2 + \frac{\partial\sigma_R}{\partial h_p}^2 \sigma_{h_p}^2 + \frac{\partial\sigma_R}{\partial z}^2 \sigma_z^2} \quad (16)$$

The expressions of the partial derivatives of σ_R , determined with the aid of Matlab symbolic derivative toolbox, are presented in Appendix A.

The σ_R uncertainty was estimated for several z values, using the same procedure adopted before to estimate the plastic layer depth uncertainty. In the graphic of Fig. 6, the vertical bars, with lengths equal to the respective σ_R value, are plotted around the coordinates of the residual stress. Considering the bounded region delimited by those bars, it is easy to construct the residual stress profile uncertainty envelope.

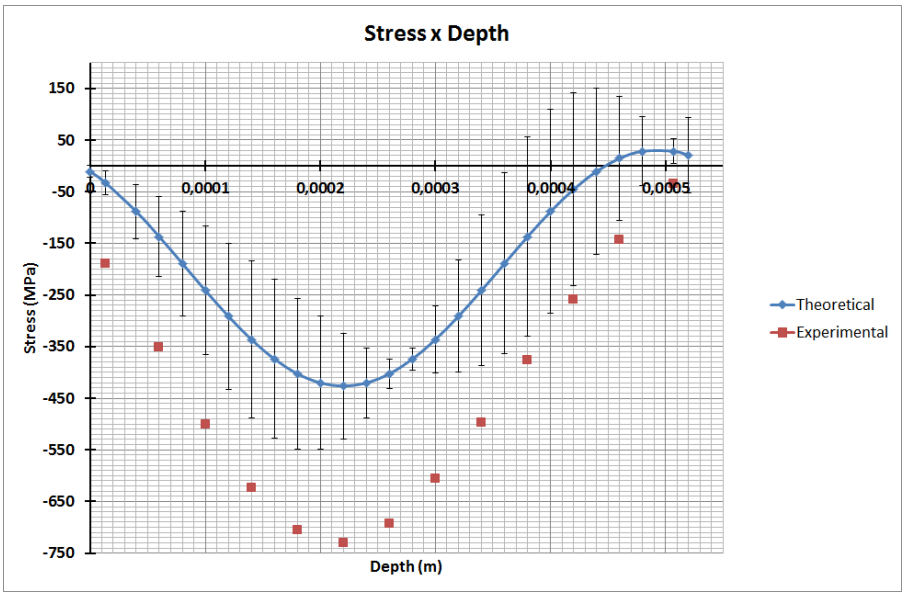

Figure 3: Stress Profile with error bars

Observing the graphic above, it is quite clear that the experimental values do not belong to the uncertainty envelope of the theoretical residual stress profile. So, the models of Al-Obaid and Hasegawa did not match the experimental residual stress measurements focused in this project. Such a discrepancy could be explained by the fact that Al-Obaid's

ISSN 2176-5480

model main focus was to explain the phenomena involved in steel plate indentation; by applying the same model to an aluminum alloy work piece could induce the differences observed.

The results of applying sensibility analysis for each point of the residual stress profile showed that geometric proprieties of the plate, such as length, thickness and the final arc height, were the ones that most influence the residual stress estimations. Also, shot radius is likely relevant, followed by the Young modulus and the impact velocity. The least relevant parameters in this case were the shot density, the Poisson's ratio and the impact pressure.

5. CONCLUSIONS

The residual stress predicted by the theoretical model didn't match the experimental data, even when considering the propagation of errors due to the uncertainty of the measured variables. However, Al-Obaid's (1995) model was conceived to be applied on steel plates while the test specimen focused in this article were made on an aluminum alloy, a factor that could give rise to the discrepancies observed in the graphic of Fig.6

On the other hand, the theoretical model predicts the shape of the stress profile and the plastic-layer depth with remarkable precision. Actually, the model shows that the residual stress exhibits a cosine profile inside the plastic zone, changing from compressive stress to traction at z=0.5mm.

Also, the sensibility analysis has shown the hierarch of the variables, being the geometrical proprieties of the peened panel the most relevant, followed by the shot dimensions. This way, when executing peen forming it is necessary to control and determine such parameters to achieve the desired results. Therefore, when performing shot peening, one must be sure of the dimensions of the peened surface, if they are precise and correct according to the project requirements. Also, taking good care when choosing the shot dimensions and type is an important part of the process, mostly because as shown in this research, this step could avoid inducing divergence in the desired results.

6. REFERENCES

Al-Obaid, Y.F., 1995, "Shot peening mechanics: experimental and theoretical analysis". *Mechanics of Materials*, n. 19, pp. 251-260.

Almeida, R.Z.H., Fleury, A.T., Martins, F.P.R., 2008, "Planejamento de trajetórias de jateamento para obtenção de cobertura uniforme em processos de peen forming". In *Anais do 5º Congresso Nacional de Engenharia Mecânica – CONEM-2008*. Salvador, Brasil.

Delijaicov, S., Fleury, A.T., Martins, F.P.R., 2010, "Application of multiple regression and neural networks to synthesize a model for peen forming process planning". *Journal of Achievements in Materials and Manufacturing Engineering*, v. 43, 2, pp. 651-656.

Evans, R.W., 2002, "Shot peening process: modeling, verification and optimization". *Materials Science and Technology*, v.18, pp. 831-839.

Fleury, A.T., Martins, F.P.R., Almeida, R.Z.H., Szilagy, G., Delijaicov, S., Pavanello, R., Button, S.T., Bravo, C.M.A.A., Gonçalves, M., Ponge-Ferreira, W.A., Braga, A.P.V., 2011, "Modelagem, simulação e validação experimental de processos de peen forming em placas de ligas de alumínio". In *Anais do 6º Congresso Brasileiro de Engenharia de Fabricação – COBEF-2011*. Caxias do Sul, Brasil.

Fleury, A.T., Delijaicov., S., Martins, F.P.R., 2009, "Residual stresses induced by peen forming processes applied to conform aluminum alloy plates". In *Proceedings of the 20th International Congress of Mechanical Engineering – COBEM-2009*. Gramado, Brazil.

Johnson, K. L., 1985, *Contact Mechanics*. Cambridge University Press, New York.

Levers, A., Prior, A., 1998, "Finite element analysis of shot peening". *Journal of Materials Processing Technology*, pp. 304-308.

Meguid, S.A., Shagal, G., Stranart, J.C., Daly, J., 1999, "Three-dimensional dynamic finite element analysis of shot-peening induced residual stresses". *Finite Element in Analysis and Design*, 31, pp. 179-191.

Meguid, S.A., Shagal, G., Stranart, J.C., 1999, "Finite element modeling of shot-peening residual stresses". *Journal of Materials and Processing Technology*, vol. 92, n. 93, pp. 401-404.

Meo, M.,Vignejevic, R., 2003, "Finite element analysis of residual stress induced by shot peening processes". *Advances in Engineering Software*, n.34, pp. 569-575.

Niku-Lari, A., 1981a, "Shot Peening". In *Proceedings of the 1st International Conference on Shot Peening*. Paris, France.

Niku-Lari, A., 1981b, "Méthode de la fléche – Méthode de la source de contraintes residuelles". In *Proceedings of the 1st International Conference on Shot Peening*. Paris, France.

Ramati, S., Levasseur, G., Kennersnecht, S., 1999, "Single piece wing skin utilization via advanced peen forming technology". In Proceedings of the 7th International Conference on Shot Peening. Warsaw, Poland.

Tatton, R.J.D., 1986, "Shot peen forming". In *Proceedings of the Impact Surface Treatment - The 2nd International Conference on Impact Treatment Processes.* Bedford, UK.

Timoshenko, S., Goodier, J.N., 1970, "Theory of Elasticity". McGraw-Hill, New York, 3rd edition.

ISSN 2176-5480

Valente, T., Bartuli, C., Sebastiani, M., Loreto, A., 2005, "Implementation and development of the incremental hole drilling method for the measurement of residual stress in thermal spray coatings". *Journal of Thermal Spray Technology*, v. 14, n. 4, pp. 462-470.

Vieira, L.C., Almeida, R.Z.H., Martins, F.P.R., Fleury, A.T., 2010, "Application of computer vision methods to estimate the coverage of peen formed plates". *Journal of Achievements in Materials and Manufacturing Engineering*, v. 43, n. 2, pp. 743-749.

Watanabe, Y., Hasegawa, N., 1995, "Simulation of Residual Stress Distribution". In *Proceedings of the 6th International Conference on Shot Peening – ICSP-6.* San Francisco, USA.

Appendix A

$$\frac{\partial \sigma_R}{\partial E} = \frac{\varepsilon_m}{1-\nu}\left[\frac{12\lambda}{\pi h}(1-\alpha)\left(\frac{h}{2}-z\right)C_1 + \frac{2\lambda}{\pi}(1-\alpha)C_2 - \frac{\epsilon(z)}{\varepsilon_m}\right]$$

$$\frac{\partial \sigma_R}{\partial \nu} = \frac{E\varepsilon_m}{(1-\nu)^2}\left[\frac{12\lambda}{\pi h}(1-\alpha)\left(\frac{h}{2}-z\right)C_1 + \frac{2\lambda}{\pi}(1-\alpha)C_2 - \frac{\epsilon(z)}{\varepsilon_m}\right]$$

$$\frac{\partial \sigma_R}{\partial \delta} = \frac{\pi E h^2}{L^2(1-\alpha)h_p C_1(1-\nu)}\left[\frac{12\lambda}{\pi h}(1-\alpha)\left(\frac{h}{2}-z\right)C_1 + \frac{2\lambda}{\pi}(1-\alpha)C_2 - \frac{\left(1+\cos\left(\frac{\pi(z-\alpha h_p)}{h_p(1-\alpha)}\right)\right)}{2}\right]$$

$$\frac{\partial \sigma_R}{\partial L} = -\frac{2\pi E\delta h^2}{L^3 h_p(1-\alpha)(1-\nu)C_1}\left[\frac{12\lambda}{\pi h}(1-\alpha)\left(\frac{h}{2}-z\right)C_1 + \frac{2\lambda}{\pi}(1-\alpha)C_2 - \frac{\left(1+\cos\left(\frac{\pi(z-\alpha h_p)}{h_p(1-\alpha)}\right)\right)}{2}\right]$$

$$\frac{\partial \sigma_R}{\partial z} = \frac{\pi E\delta h^2}{L^2 h_p(1-\alpha)(1-\nu)C_1}\left[\pi\left(\frac{\sin\left(\frac{\pi(z-\alpha h_p)}{h_p(\alpha-1)}\right)}{2h_p(\alpha-1)}\right) - \frac{12h_p(1-\alpha)C_1}{\pi h^2}\right]$$

$$\frac{\partial \sigma_R}{\partial h_p} = -\frac{\pi E\delta h^2 A}{L^2 h_p^2(\alpha-1)(\nu-1)C} - \frac{\pi E\delta h^2\left[\frac{\left(2\left(\sin\left(\frac{\pi\alpha}{2(\alpha-1)}\right)-1\right)(\alpha-1)\right)}{\pi h} - \sin\left(\frac{\pi(z-\alpha h_p)}{h_p(\alpha-1)}\right)\left(\frac{\pi(z-\alpha h_p)}{h_p^2(\alpha-1)} + \frac{\pi\alpha}{h_p(\alpha-1)}\right) + \left(\frac{12\left(\frac{h}{2}-z\right)(\alpha-1)}{\pi h^2}\right)(C+Bh_p)\right]}{L^2 h_p(\alpha-1)(\nu-1)C} - \frac{\pi E\delta h^2 BA}{L^2 h_p(\alpha-1)(\nu-1)C^2}$$

With:

$$A = \frac{\cos\left(\frac{\pi(z-\alpha h_p)}{h_p(\alpha-1)}\right)}{2} - \frac{2h_p\left(\sin\left(\frac{\pi\alpha}{2(\alpha-1)}\right)(\alpha-1)\right)}{\pi h} - \frac{12h_p\left(\frac{h}{2}-z\right)(\alpha-1)C}{\pi h^2} + \frac{1}{2}$$

$$B = \frac{2}{h} + \frac{4\cos\left(\frac{\pi\alpha}{2(\alpha-1)}\right)(\alpha-1)}{\pi h}$$

$$C = \sin\left(\frac{\pi\alpha}{2(\alpha-1)}\right) + \frac{2h_p}{h} + \frac{4h_p\cos\left(\frac{\pi\alpha}{2(\alpha-1)}\right)(\alpha-1)}{\pi h} - 1$$

$$\frac{\partial \sigma_R}{\partial h} = \frac{\pi E\delta h^2\left[\frac{G}{\pi h^2} - \frac{6h_p(\alpha-1)H}{\pi h^2} + \frac{12h_p\left(\frac{h}{2}-z\right)(\alpha-1)E}{\pi h^2} + \frac{24h_p\left(\frac{h}{2}-z\right)(\alpha-1)H}{\pi h^3}\right]}{F} + \frac{2\pi E\delta hD}{F} + \frac{\pi E\delta h^2 DE}{L^2 h_p(\alpha-1)(\nu-1)H^2}$$

With:

$$D = \frac{\cos\left(\frac{\pi(z-\alpha h_p)}{h_p(\alpha-1)}\right)}{2} - \frac{G}{\pi h} - \frac{12h_p\left(\frac{h}{2}-z\right)(\alpha-1)H}{\pi h^2} + \frac{1}{2}$$

$$E = \frac{2h_p}{h^2} + \frac{I}{\pi h^2}$$

$$F = Lh_p(\alpha-1)(\nu-1)H$$

$$G = 2h_p\left(\sin\left(\frac{\pi\alpha}{2(\alpha-1)}\right)-1\right)(\alpha-1)$$

$$H = \sin\left(\frac{\pi\alpha}{2(\alpha-1)}\right) + \frac{2h_p}{h} + \frac{I}{\pi h} - 1$$

$$I = 4h_p cos\left(\frac{\pi\alpha}{2(\alpha-1)}\right)(\alpha-1)$$

7. RESPONSIBILITY NOTICE

The authors are the only responsible for the printed material included in this paper.